Synaptic noise in neural networks at finite temperatures

1993 J. Phys. A: Math. Gen. 26 3697

(http://iopscience.iop.org/0305-4470/26/15/019)

J. Phys. A: Math. Gen. 26 (1993) 3697–3705. Printed in the UK

Synaptic noise in neural networks at finite temperatures

M Y Choi†§, K Park‡ and G M Shim‡||

† Department of Physics, University of Washington, Seattle, WA 98195, USA

‡ Department of Physics, Seoul National University, Seoul 151-742, Korea

Received 16 February 1993, in final form 10 May 1993

Abstract. We investigate the effects of the synaptic noise in neural networks at finite temperatures. The analytic results are obtained through the use of the path-integral formulation which facilitates performing the quenched average over the random patterns and random noises. We consider the noise effects in the diluted Hopfield model, the fully-connected Hopfield model and the dynamic model, laying emphasis on the interplay with the temperature. In the phase diagrams drawn as functions of the temperature, the storage, and the noise strength, interesting features including re-entrance, first-order transitions as well as second-order transitions are found.

1. Introduction

Neural-network models attempt to explain intriguing features such as memory, learning, fault tolerance, information storage and retrieval, etc. in terms of the collective properties of the system, see, for example, [1]. In spin-glass-like models of neural networks [2–6], each neuron is usually regarded as an Ising spin with two possible states: the spin-up state ($s = +1$) or the spin-down state ($s = -1$) depending on whether the neuron is, or is not, firing an electrochemical signal. The state of the network of N such neurons is defined to be the instantaneous configuration of all the spin variables at time t. The neurons are interconnected by synaptic junctions of strength J_{ij}, which determine the contribution of the signal fired by the jth neuron to the postsynaptic potential on the ith neuron. Often the synaptic couplings are constructed of p given spin configurations according to the Hebbian rule

$$J_{ij} = \frac{1}{N}\sum_{\mu=1}^{p} \xi_i^\mu \xi_j^\mu \qquad (i \neq j) \tag{1.1}$$

where the ξ_i^μ representing p ($\equiv \alpha N$) stored patterns are regarded as quenched, independent random variables taking the values ± 1 with equal probability. This assignment allows the networks to evolve from the given initial state into one of the p stored patterns.

In general there exist fluctuations in the number of neurotransmitters released across a synapse, which necessitates a probabilistic description. Accordingly, the threshold behaviour of the ith neuron at time t is described by a probability that depends on the difference between the total potential on the ith neuron V_i and its threshold value V_0

$$V_i - V_0 = b_i + \sum_j J_{ij} s_j(t - t_d) \equiv h_i(t) \tag{1.2}$$

§ Permanent address: Department of Physics, Seoul National University, Seoul 151-742, Korea.

|| Present address: Instituut voor Theoretische Fysica, Katholieke Universiteit Leuven, B3001 Leuven, Belgium.

0305-4470/93/153697+09$07.50

where the external field $b_i \equiv \sum_j J_{ij} - V_0$ is usually assumed to vanish, and $s_j(t - t_d)$ denotes the state of the jth neuron at time $t - t_d$ with t_d being the delay in the interactions if any. This probability function contains a parameter $T(\equiv \beta^{-1})$ which plays the role of a temperature and which measures the width of the threshold region. However, the *temperature* T is not to be understood as modelling the physical temperature of a biological neural network; it effectively controls the number fluctuations of neurotransmitters while the synaptic couplings are regarded as fixed. This approach allows for the application of standard techniques of statistical mechanics.

There is also another way to consider the randomness which is unavoidable in the synaptic couplings of real biological systems. For example, we may introduce the static noise in synaptic couplings and modify (1.1) as follows

$$J_{ij} = \frac{1}{N}\sum_{\mu=1}^{p} \xi_i^\mu \xi_j^\mu + \eta_{ij} \tag{1.3}$$

where the distribution of the noise η_{ij} is, for simplicity, chosen to be a Gaussian with zero mean and variance ϵ/N. Such a type of synaptic noise has been considered in the context of the nonlinear synapse and learning [7], and analysed either at zero temperature [8] or at zero storage (i.e. in the case that only a finite number of patterns are stored) [9], displaying overall deterioration of the performance of the networks.

The purpose of this paper is to investigate the effects of such synaptic noise in neural networks *at finite temperatures and finite storages*. It is important to note here that this noise, regarded as the internal noise of the synaptic coupling itself, is introduced on a very different footing from the temperature. We use the path-integral formulation [10], which facilitates performing the quenched average over the random patterns and random noises, and consider, at finite temperatures and storages, the diluted Hopfield model [5], the fully-connected Hopfield model [3, 4], and the dynamic model [6]. In the phase diagrams drawn as functions of the temperature, the storage, and the noise strength, interesting features such as re-entrance are found, which reflect the subtle interplay between the synaptic noise and the temperature.

2. The diluted Hopfield model

The asymmetric diluted version of the Hopfield model which has been solved exactly [5] can be generalized straightforwardly to include the synaptic noise. We thus introduce the synaptic noise according to

$$J_{ij} = C_{ij}\left\{\sum_\mu \xi_i^\mu \xi_j^\mu + \eta_{ij}\right\} \tag{2.1}$$

where the C_{ij}'s are independent, random parameters following the distribution

$$\rho(C_{ij}) = \frac{C}{N}\delta(C_{ij} - 1) + \left(1 - \frac{C}{N}\right)\delta(C_{ij})$$

and compute the local field $h_i(t)$ on site i

$$h_i(t) \equiv \sum_j J_{ij} s_j(t)$$

$$= h_i^0(t) + \sum_{r=1}^{K} \eta_{ij_r} s_{j_r}(t)$$

where η_{ij} obeys a Gaussian distribution with zero mean and variance $C\epsilon$, and $h_i^0(t)$ denotes the local field without synaptic noise. Here the time delay has been disregarded ($t_d \equiv 0$), and K is the number of neurons connected with the ith neuron. Since the spins $s_{j_1}, s_{j_2}, \ldots, s_{j_K}$ are uncorrelated for almost all sites i, we may set

$$\sum_{r=1}^{K} \eta_{ij_r} s_{j_r}(t) = \sqrt{KC\epsilon}\, y_i$$

where y_i obeys a Gaussian distribution with zero mean and unit variance. We limit ourselves to the thermodynamic limit ($N \to \infty$), and consider the Mattis-state solution described by the order parameter of the form $m^\mu(t) \equiv N^{-1} \sum_{i=1}^{N} \xi_i^\mu \sigma_i(t) = m(t)\delta_{\mu 1}$, where $\sigma_i(t) \equiv \langle s_i(t) \rangle$ is the activity of the ith neuron. As long as $C \ll \log N$, we still have the exact relation

$$m(t+1) = f(m(t)) \tag{2.2}$$

where, for simplicity, the discrete time step has been set equal to unity. In the limit $C \to \infty$ and $p \to \infty$ (with $N \to \infty$ in advance), $f(m)$ at temperature $T(\equiv \beta^{-1})$ is given by

$$f(m) = \int_{-\infty}^{\infty} \frac{dz}{\sqrt{2\pi}} e^{-z^2/2} \tanh C\beta\left(z\sqrt{\alpha + \epsilon} + m\right) \tag{2.3}$$

where $\alpha \equiv (p-1)/C$ is the storage ratio. In the stationary state, we have $m = f(m)$; the critical temperature T_c is then given by $f'(0) = 1$. In the absence of the synaptic noise ($\epsilon = 0$), (2.3) obviously reduces to the corresponding equation in [5]. Accordingly, the system with synaptic noise exhibits essentially the same behaviour as that without noise, and we just need to replace α by $\alpha + \epsilon$ in the results of [5]. For example, at zero temperature, the storage capacity is given by $\alpha_c = 2/\pi - \epsilon$ for given strength of the synaptic noise, which shows the decrease of the capacity α_c due to the synaptic noise. It is also obvious that the maximum allowable noise is given by $\epsilon_c = 2/\pi$: beyond ϵ_c, only a finite number of patterns can be stored in the system.

3. The fully-connected Hopfield model

The noise effects in the fully-connected Hopfield model have been studied via the replica trick, mostly at zero temperature [8] or at zero storage [9]. Here we avoid the replica method which has some mathematical deficiencies. Instead we use the path-integral formulation [10], which allows us to perform the quenched averages over the random patterns and random noises exactly, and investigate the noise effects at finite temperatures and storages.

The scheme of [10] can be straightforwardly extended to the system with synaptic noise as given by (1.3). We consider, as usual, only a finite number of patterns ($\xi^1, \ldots, \xi^l$) to be condensed and the remaining ($p-l$) patterns to have an overlap at most of order $O(1/\sqrt{N})$. In this case the resulting extended dynamical mean-field theory leads to essentially a single neuron problem, and the local field in (1.2) can be replaced by ($t_d = 0$)

$$h(t) = \sum_\mu m^\mu \xi^\mu + \sqrt{\alpha}\Phi(t) + \sqrt{\epsilon}\Psi(t) + \alpha \int dt'\, \tilde{S}(t-t')\sigma(t') \tag{3.1}$$

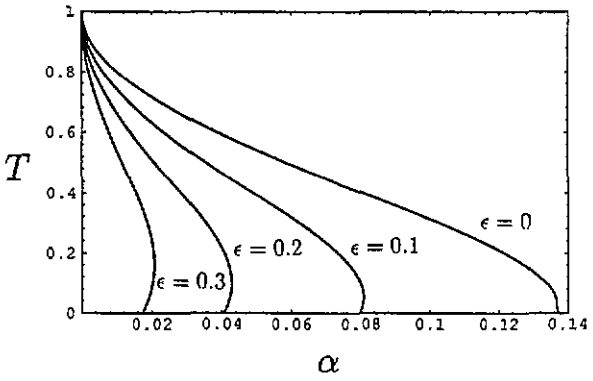

Figure 1. Phase diagram in the (T, α) plane for various values of ϵ.

where $\sigma(t)$ is the activity of a single neuron, and m^μ describes the overlap between the network and the condensed memory μ. In (3.1), $\Phi(t)$ and $\Psi(t)$ are Gaussian random fields with zero mean and correlations

$$\langle \Phi(t)\Phi(t') \rangle_\Phi = R(t-t') \qquad \langle \Psi(t)\Psi(t') \rangle_\Psi = C(t-t')$$

and

$$\tilde{S}(t-t') \equiv \frac{\mathrm{i}}{\alpha} S(t-t') - \delta(t-t') - \frac{\epsilon}{\alpha} G(t-t')$$

where $C(t)$ and $G(t)$ are the autocorrelation and response functions, while $R(t)$ and $S(t)$ are the random overlap correlation and response functions, respectively.

To extract the equilibrium properties of the model, we consider the activity as well as the macroscopic overlaps to be time-independent, and define the static order parameters as the long-time limit of the autocorrelation and the random overlap correlation: $q \equiv \lim_{t\to\infty} C(t)$ and $r \equiv \lim_{t\to\infty} R(t)$, which are the Edward–Anderson order parameter and the mean square random overlap, respectively. This finally leads to the static order parameter equations for the ideal Mattis state

$$m = \langle\!\langle \tanh \beta \left(z\sqrt{\alpha r + \epsilon q} + m \right) \rangle\!\rangle \tag{3.2a}$$

$$q = \langle\!\langle \tanh^2 \beta \left(z\sqrt{\alpha r + \epsilon q} + m \right) \rangle\!\rangle \tag{3.2b}$$

$$r = \frac{q}{[1-\beta(1-q)]^2} \tag{3.2c}$$

where $\langle\!\langle\ \rangle\!\rangle$ denotes the Gaussian average over stochastic variable z.

Equations (3.2) have been also derived via the replica method [8], and analysed mostly in the zero temperature limit ($\beta \to \infty$). In this limit, as ϵ is increased from zero, the storage capacity α_c gets smaller, eventually approaching zero as $\epsilon \to \epsilon_c = 2/\pi$. The corresponding zero-temperature phase boundary in the (ϵ, α) plane constitutes a first-order transition line. On the other hand, at zero storage ($\alpha = 0$) and for $\epsilon > \epsilon_c$, the network can retrieve the pattern only at finite temperatures. This apparently indicates that probabilistic (rather than deterministic) operation of the network is advantageous in the presence of synaptic noise, which should be inevitable in the real system. From a different point of view, the synaptic noise may be interpreted as incompleteness of the pattern, causing a deterioration in the performance of the network to recall the imbedded pattern.

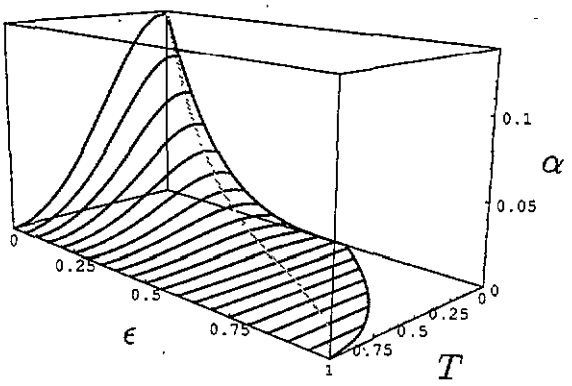

Figure 2. Overall phase diagram in the (T, α, ϵ) space.

Figure 1 is the phase diagram in the (T, α) plane for various values of the noise strength ϵ, exhibiting that the storage capacity of networks shrinks rapidly as the noise grows. It displays interesting re-entrant behaviour in the presence of synaptic noise. This obviously implies that the network can store more patterns at finite temperatures than at zero temperature, again suggesting that probabilistic operation is desirable. This re-entrance appears to reflect the subtle interplay between the synaptic noise and the temperature measuring the uncertainty in the threshold behaviour of a neuron. The overall phase diagram in the (T, α, ϵ) space as determined by the solutions of (3.2) is shown in figure 2. The gray line connects points where the storage capacity α_c reaches its maxima.

The network also exhibits spin-glass properties outside the memory-retrieval phase. To find the spin-glass transition temperature T_g, we expand (3.2) in powers of q and r, setting $m = 0$. The transition temperature is, to the leading order, determined by

$$q \approx \beta^2(\alpha r + \epsilon q)$$
$$\approx \beta^2 q \left\{ \frac{\alpha}{(1-\beta)^2} + \epsilon \right\}$$

which yields

$$\alpha T_g^2 + \epsilon(T_g - 1)^2 = T_g^2(T_g - 1)^2. \tag{3.3}$$

In the absence of noise ($\epsilon = 0$), this gives the well-known result

$$T_g = 1 + \sqrt{\alpha} \tag{3.4}$$

while T_g increases continuously as ϵ grows. The corresponding phase boundary is shown in figure 3, for $\epsilon = 0.5$ and 1 as well as for $\epsilon = 0$.

4. The dynamic model

The dynamic model for neural networks explicitly takes into account the existence of several time scales without discretizing the time [6]. It does not possess a Hamiltonian, necessitating dynamic analysis such as the path-integral approach. The application of the

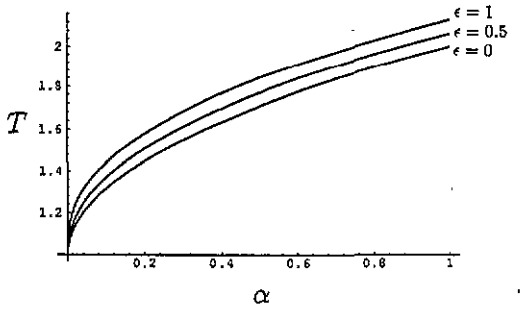

Figure 3. Spin-glass phase boundaries for $\epsilon = 0$, 0.5 and 1.

path-integral method has been done in the absence of synaptic noise [11], and again the corresponding dynamic mean-field theory can be straightforwardly extended to the system with noisy synaptic couplings. It eventually leads to the following equations for the static order parameters

$$m^\mu = \langle\!\langle \xi^\mu M_z \rangle\!\rangle \tag{4.1a}$$

$$q = \langle\!\langle M_z^2 \rangle\!\rangle \tag{4.1b}$$

$$r = \frac{q}{\{1 - \langle\!\langle \partial M_z / \partial h_z \rangle\!\rangle\}^2} \tag{4.1c}$$

where $\langle\!\langle\ \rangle\!\rangle$ denotes the average over both the random patterns $\{\xi^\mu\}$ and the Gaussian variable z, and

$$M_z \equiv \frac{1 - 2a + \tanh \beta h_z}{1 + 2a + \tanh \beta h_z}$$

with

$$h_z \equiv z\sqrt{\alpha r + \epsilon q} + \sum_{\mu=1}^{l} \xi^\mu m^\mu.$$

We again investigate the Mattis-state solution of the order-parameter equation (4.1). In the absence of the synaptic noise ($\epsilon = 0$), the phase diagram displayed by (4.1) has been obtained in the (T, α, a) space [11], where a is the ratio of the refractory period to the action potential duration. Here we concentrate on the effects of the synaptic noise, and first consider the zero-temperature ($T = 0$) limit. We introduce the parameter $u \equiv m/\sqrt{2(\alpha r + \epsilon q)}$, and write equations (4.1) in the single form

$$u = \frac{\operatorname{erf}(u)\left[\operatorname{erf}(u) - 2ue^{-u^2}/\sqrt{\pi}\right]}{\sqrt{1 + a^2}\left(2\alpha \operatorname{erf}^2(u) + 2\epsilon\left[\operatorname{erf}(u) - 2ue^{-u^2}/\sqrt{\pi}\right]^2\right)^{1/2}} \tag{4.2}$$

where $\operatorname{erf}(x)$ is the error function. The corresponding phase diagram in the (a, α, ϵ) space is shown in figure 4, where the phase boundary in the $a = 0$ plane coincides with the zero-temperature phase diagram of the Hopfield model.

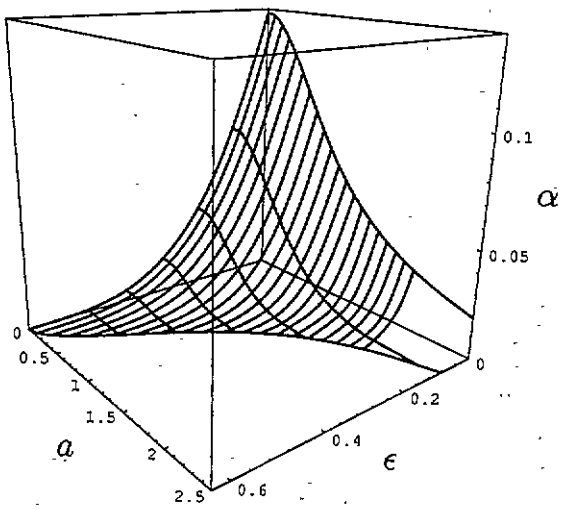

Figure 4. Zero-temperature phase diagram in the (a, α, ϵ) space.

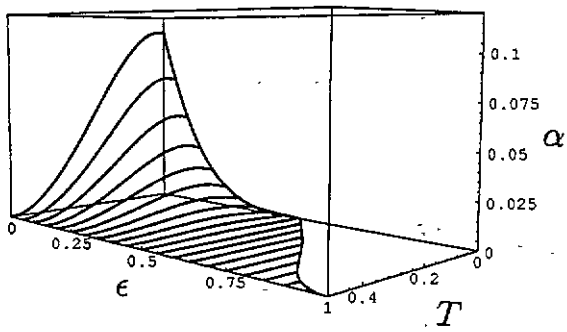

Figure 5. Phase diagram in the (T, α, ϵ) space for $a = 1/2$.

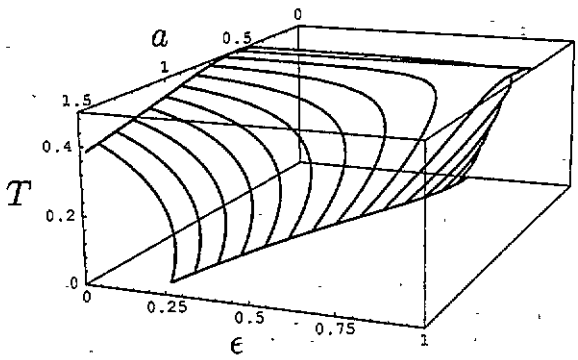

Figure 6. Phase diagram in the (T, ϵ, a) space for $\alpha = 0$.

At finite temperatures, we may draw the phase diagrams for given values of a in the (T, α, ϵ) space; they show some difference according to whether a is equal to $1/2$ or not.

In figure 5, the phase diagram in the (T, α, ϵ) space for $a = 1/2$ is plotted, which displays properties qualitatively similar to those of the Hopfield model. Thus the upper critical temperature for pattern retrieval remains unaffected by the synaptic noise, i.e. $T_c = 1/2$. For $a \neq 1/2$, in contrast, this is not the case, and figure 6 shows how the phase boundary in the $\alpha = 0$ plane depends on the value of a: the phase boundary forms a smooth surface except at $a = 1/2$ while for $a = 1/2$, it extends to $\epsilon = 1$ with constant upper critical temperature ($T_c = 1/2$) as also shown in figure 5. In the latter case ($a = 1/2$), the phase boundary displays a cusp singularity at $(T, \epsilon) = (1/2, 1)$.

We now investigate more carefully this qualitative difference between the two cases ($a = 1/2$ and $a \neq 1/2$) in the pattern-retrieval phase boundary. In [6], the simple case of zero storage without noise ($\alpha = \epsilon = 0$) has been studied, and for $a > a_c \equiv (\sqrt{3} - 1)/2$, the continuous transition line $T_c(\alpha = \epsilon = 0) \equiv T_0(\equiv \beta_0^{-1})$ has been found to be given by $\beta_0 = (1 + 2a)^2/4a$. When ϵ is small, the macroscopic overlap m is expected to be small in the vicinity of the transition line. Searching for non-zero solutions for m, we thus expand the Mattis-state solution of equations (4.1) in small parameters m, ϵ and $t \equiv (\beta/\beta_0 - 1)$

$$t = A(\tfrac{1}{3}m^2 + \epsilon q) \tag{4.3a}$$

$$q = \left[\frac{1-2a}{1+2a}\right]^2 + \left[2 - \frac{1}{2a}\right](m^2 + \epsilon q) \tag{4.3b}$$

with $A \equiv \beta_0(2a^2 + 2a - 1)/(2a)$. When $a \neq 1/2$, the Edward–Anderson order parameter q is of the order of unity, and the transition temperature below which non-zero m exists follows from (4.3a)

$$\frac{T_c(\epsilon)}{T_0} = 1 - A\left(\frac{1-2a}{1+2a}\right)^2 \epsilon. \tag{4.4}$$

On the other hand, for $a = 1/2$, the first term on the right-hand side of (4.3b) vanishes, and the transition temperature is unaffected by the noise. In fact the transition temperature is given by $T_c(\epsilon) = T_0(a = 1/2) = 1/2$ all the way to $\epsilon = 1$. Thus the origin of the difference between the two cases in the memory-retrieval phase boundary again traces back to the spin-up–spin-down symmetry of the network, similarly to the case without noise ($\epsilon = 0$) [11].

5. Conclusion

We have studied effects of the static synaptic noise in several neural network models such as the diluted Hopfield model, the fully-connected Hopfield model, and the dynamic model. The synaptic noise is treated as quenched random variables with a Gaussian distribution, and the path-integral formulation has been applied as a convenient approach to the fully-connected model without the self-averaging property. The phase diagrams have been obtained as functions of the temperature T, the storage α, the noise strength ϵ, and, in the case of the dynamic model, the ratio a of the refractory period to the action-potential duration. In the case of the fully-connected Hopfield model, the phase diagram reduces to the known results in the appropriate limits. In addition, the diagrams obtained display quite new features, manifesting the subtle interplay between the two kinds of noise present in the system. In particular, the interesting possibility of re-entrance has been pointed out. There are several points for further study, particularly in the dynamic model, where the short-time parts have been assumed irrelevant to the static properties without clear justification. The case $a = 1/2$ also deserves some attention, for there exists qualitative difference owing to the presence of the spin-up–spin-down symmetry.

Acknowledgments

We are grateful to D Kim for stimulating discussions and to H Jeong for his help with the computer work. This work was supported in part by the Ministry of Education of Korea, and in part by the Korea Science and Engineering Foundation through a grant to the Center for Theoretical Physics, Seoul National University.

References

[1] Peretto P 1992 *An Introduction to the Modeling of Neural Networks* (Cambridge: Cambridge University Press)
1989 *J. Phys. A: Math. Gen.* **22** various articles
[2] Little W A 1974 *Math. Biosci.* **19** 101
Little W A and Shaw G A 1978 *Math. Biosci.* **39** 281
[3] Hopfield J J 1982 *Proc. Nat. Acad. Sci. USA* **79** 2554
[4] Amit D J, Gutfreund H and Sompolinsky H 1985 *Phys. Rev.* A **32** 1007; 1985 *Phys. Rev. Lett.* **55** 1530
[5] Derrida B, Gardner E and Zippelius A 1987 *Europhys. Lett.* **4** 167
[6] Choi M Y 1988 *Phys. Rev. Lett.* **61** 2809
[7] van Hemmen J L and Kühn R 1986 *Phys. Rev. Lett.* **57** 913
Fontanari J F and Meir R 1989 *Phys. Rev.* A **40** 2806
[8] Sompolinsky H 1986 *Phys. Rev.* A **34** 2571; 1987 *Heidelberg Colloquium on Glassy Dynamics* ed J L van Hemmen and I Morgenstern (Berlin: Springer)
[9] van Hemmen J L and Rzazewski K 1987 *J. Phys. A: Math. Gen.* **20** 6553
[10] Sommers H J 1987 *Phys. Rev. Lett.* **58** 1268
Rieger H, Schreckenberg M and Zittartz J 1988 *Z. Phys.* B **72** 523
[11] Shim G M, Choi M Y and Kim D 1991 *Phys. Rev.* A **43** 1079